

E Joffrin et al

MHD Internal Transport Barrier Triggering in Low Positive Magnetic Shear Scenarios in JET

MHD Internal Transport Barrier Triggering in Low Positive Magnetic Shear Scenarios in JET

E Joffrin¹, C D Challis, T C Hender,
D F Howell, G T A Huysmans¹.

EURATOM/UKAEA Fusion Association, Culham Science Centre,
Abingdon, Oxfordshire, OX14 3DB, UK.

¹Association Euratom-CEA pour la fusion, CEA Cadarache,
F-13108, St. Paul lez Durance, France

“This document is intended for publication in the open literature. It is made available on the understanding that it may not be further circulated and extracts or references may not be published prior to publication of the original when applicable, or without the consent of the Publications Officer, EFDA, Culham Science Centre, Abingdon, Oxon, OX14 3DB, UK.”

“Enquiries about Copyright and reproduction should be addressed to the Publications Officer, EFDA, Culham Science Centre, Abingdon, Oxon, OX14 3DB, UK.”

MHD Internal Transport Barrier Triggering in Low Positive Magnetic Shear Scenarios in JET

E. Joffrin¹, C.D. Challis², T.C. Hender²,
D.F. Howell², G.T.A. Huysmans¹

¹*Association Euratom-CEA pour la fusion, CEA Cadarache,
F-13108, St. Paul lez Durance, France*

²*Euratom/UKAEA Fusion Association, Culham Science Centre,
Abingdon, Oxon, OX14 3DB, UK.*

ABSTRACT

Internal Transport Barriers (ITB) can be produced in JET by the application of strong additional heating during the current rise of the plasma discharge. These ‘so-called’ Optimised Shear (OS) experiments with low positive magnetic shear have revealed a strong dependence between the formation of the barrier and integer q magnetic surfaces ($q=2$ or $q=3$). Further analysis also shows a correlation between the emergence of the ITB and edge external MHD, which is triggered when an integer q surface occurs at the edge of a strongly heated plasma ($q=4$, $q=5$ or $q=6$). Mode coupling is the prime candidate to explain the link between the internal integer flux surfaces, where the ITB is triggered, and the plasma edge. Modelling of the magneto-hydrodynamic (MHD) behaviour confirms the possibility of such a mechanism. Once coupled, this destabilised mode is thought to enhance locally the EXB shearing rate, either by magnetic ‘braking’ or by the radial transport losses resulting from the modification of the field line topology. This could then trigger the ITB inside the internal integer surface at $q=2$ or $q=3$.

INTRODUCTION

In recent years, the performance in terms of confinement and fusion yield of several tokamaks (DIII-D [1], JT60-U [2], TFTR [3], Tore Supra [4], ASDEX [5] and JET [6]) has been significantly increased by forming a core region of reduced anomalous transport called an Internal Transport Barrier (ITB). These regimes which are promising for future tokamak operation, are generally triggered when the plasma is heated with various amounts and combinations of Neutral Beam Injection (NBI) and Ion Cyclotron Resonance Heating (ICRH) during the ramp-up phase of the plasma current. To extrapolate these improved regimes to larger sized tokamaks and reactors with lower power density from external sources, it is essential to determine the minimum required power to access these regimes and, therefore, the triggering conditions to form an ITB must be identified. Furthermore, the physics understanding of ITB triggering mechanisms will assist the ultimate goal of actively controlling the onset, duration and confinement resulting from the formation of ITBs in advanced tokamak plasmas.

Studies of the ITB formation process have remained an important part of the JET Optimised Shear programme [7]. The reduction of transport in JET is associated with localised turbulence suppression [8] and correlates with both plasma flow shearing rate [9] and magnetic shear [10]. Analysis has also revealed links between integer q surfaces and ITBs. A series of experiments designed to vary the location of these surfaces in a low magnetic shear region [11] has shown that the $q=2$ and $q=3$ surfaces play a major role in the formation of the barrier. The link between ITBs and rational magnetic surfaces has also been reported on other devices such as JT60-U [12], DIII-D [13] and RTP [14]. Experiments also show that the sensitivity to the integer q surfaces seems to decrease as the input power is raised. The power to produce ITBs, also referred to as the power ‘threshold’, seems therefore to be dependent on the current density profile.

In this paper, the experimental evidence is shown for the link between integer q surfaces and the ITB formation, and the link between an edge integer flux surface and the ITB trigger. From this analysis, a new candidate mechanism is put forward to explain the triggering of ITBs in JET which is consistent with the observation of a sensitivity of the power threshold for the ITB formation to the location of integer q surfaces. Mode coupling between edge integer and internal integer q surfaces is analysed both experimentally and by theory modelling. This mode coupling process appears a good candidate to explain the origin of the triggering of ITBs in JET discharges with low central magnetic shear.

ROLE OF INTERNAL INTEGER Q SURFACES IN THE ITB FORMATION.

In JET, Optimised Shear experiments [15] are conducted in divertor configurations by heating large volume plasmas during the current rise. ITBs are achieved at various toroidal magnetic field strengths (1.7T, 2.6T, 3.0T or 3.4T) using a current ramp-up rate of about 0.35-0.45MA/s and reaching 1.8MA to 3.5MA at the plateau. The creation of the ITBs is very sensitive to the additional heating power level and timing. This additional power is composed of NBI and ICRH whose resonance frequency is selected to provide hydrogen minority fundamental heating close to the plasma centre. In general for low core magnetic shear, the presence of the $q=2$ surface appears to be a necessary condition for the formation of ITBs [7].

An experiment designed to vary the location of rational q surfaces within the plasma has clearly shown a link between integer rational surfaces and ITB formation. In this experiment, performed with a magnetic field strength of 2.6T, the time of the main heating pulse (10.5MW of neutral beam heating and 5MW of ion resonance heating) is scanned during the current rise [11] (fig 1). Due to the high additional heating power, the current profile is essentially frozen when the main heating pulse is applied (characterised by the time t_{heat} as shown in figure 1).

In this paper, ITBs are identified in location and onset time using the electron temperature measurements from an ECE heterodyne radiometer. ITBs are usually characterised by the discontinuity in the slope of the electron and ion temperature profiles resulting in a strong rise of the fusion yield due to reactions between deuterium ions in the plasma and NBI. In this paper, the ITB onset time and its foot point location are determined using a specific criterion based on

the parameter $\rho^*_T = \rho_s / L_T$, where L_T is the electron temperature gradient length and ρ_s the electron Larmor radius [16]. This parameter compares the drift wave scale length ρ_s to the local temperature gradient scale length. It is experimentally found that an ITB is formed when ρ^*_T exceeds $1.4 \cdot 10^{-2}$. This criterion has proven its efficiency to identify in time and space the presence of an ITB in JET plasmas at different magnetic fields and in a large variety of plasma conditions (different magnetic field strength, plasma current and current ramp-up rate). The spatial and temporal resolution of the ECE diagnostic is sufficiently high that location of the outermost edge of the ITB, or ‘foot-point’, and its onset time can be determined within ± 3 cm and ± 100 ms, respectively.

Motional Stark Effect (MSE) [17] measurements have been made at the target time t_{heat} . These data have been included in the equilibrium reconstruction code, EFIT [18], to infer the q profile and to follow its evolution as the heating time is varied.

Several types of barrier are observed when varying t_{heat} (fig 1). High performance ITBs (characterised by a high neutron yield) are only encountered in a very narrow range of t_{heat} corresponding to a target central safety factor q_0 very close to 2 (fig 2a). In this case the barrier forms very promptly at a radius $R=3.35$ m and the neutron yield reaches $1.4 \cdot 10^{16}$ neutrons per second. When the barrier forms the ratio between kinetic and poloidal magnetic pressures β_p ranges from 0.3 to 0.4 and the volume average density prior to the main heating is about $1.0 \cdot 10^{19} \text{ m}^{-3}$. With later heating, and therefore at lower target q_0 , ‘weaker’ ITBs are formed at a wider radius (typically 3.5m), consistent with the altered location of the $q=2$ surface (fig 2b). Early heating (with q_0 higher than 2) can produce a very wide ITB (‘foot-point’ at $R=3.65$ m), indicating a possible link with the $q=3$ surface this time (fig 2c).

This link is indeed confirmed statistically when comparing the ITB ‘foot-point’ location with the position of the $q=3$ surface determined using the EFIT equilibrium code for a database of seven different discharges with different levels of additional heating and magnetic field strength (2.6T and 3.4T). Because the $q=3$ surface is close to the plasma edge, the location of this surface can be determined with a relatively good accuracy (5cm) even without internal flux measurements, such as MSE or polarimetry. Figure 3 shows that the $q=3$ surface lies systematically outside the ITB ‘foot-point’. This is very similar to the observations reported from [12] for weak positive shear where the ‘foot-point’ of the barrier seems to coincide with the location of the $q=3$ surface.

To summarise this timing scan experiment, figure 4 shows t_{heat} as function of the location of the ITB as measured by the criterion for each discharge. The optimum point in the scan is clearly observed for a very precise timing of 3.3s. For this specific timing the pulses are producing the highest neutron yield (in the range of $1-1.5 \cdot 10^{16}$ neutrons/s). For late timing, and therefore when q_0 decreases, the barriers are ‘weaker’ (in terms of neutron yield) but also broader and eventually cannot be triggered when the $q=2$ surface becomes too wide. For early timing, $q=2$ barriers cannot be formed because the $q=2$ surface is not yet present but wide barriers are observed to correlate with the $q=3$ surface.

In this experiment, it is important to note that either prompt ITBs or a local flattening of the electron temperature profile is observed at the optimum timing. This ‘flattening’ is correlated with an $n=1$ $m=2$ MHD activity and thus, associated with the presence of a core $q=2$ island growing in the low shear region near the plasma centre and preventing the growth of the ITB. At the optimum timing and because of the flat q profile, the $q=2$ surface could be located either in a region of very low shear (thus encouraging the development of a large island) or more off-axis in larger positive shear region. This MHD $q=2$ event also confirms that q_0 is indeed close to 2 at the optimum timing.

From the above analysis, it appears that the creation of $q=2$ or $q=3$ ITBs at constant power is closely linked to the heating time. The level of additional heating power required to trigger an ITB also depends on the heating time. As the target q profile evolves (i.e. q reduces) more power is required to trigger a ‘strong’ ITB. To illustrate this point a large database of 3.4T ITBs has been built up. At this magnetic field and at the lowest heating power at which an ITB is observed (20MW), figure 5 shows the same trend as at 2.6T, and barriers can only be formed in a very narrow range of target q profiles when q_0 is very close to 2. This very localised peak in neutron yield observed when q_0 is close to 2 suggests that the q profile, and in particular the location of the $q=2$ surface, is essential for the ITB trigger. As the target q_0 is decreased, and the $q=2$ surface widens, more power is required to form an ITB. At the highest power level shown (24MW), the domain of existence of ITBs is much less sensitive to the precise value of q_0 . This suggests that the central pressure or flow shear inside the $q=2$ surface is another key parameter to trigger the ITBs. It should be noted that the target q profile, and in particular the central magnetic shear, can vary in the different pulses in figure 5. In fact recent experiments [11] have demonstrated that the required power to trigger an ITB can be significantly lowered by reversing the central magnetic shear with Lower Hybrid Current Drive in the current ramp-up phase. However, in all the results presented here LHCD is not used during the pre-heat and only modest (on-axis) ICRH pre-heat power (less than 2MW) is used which does not affect significantly the q profile evolution.

ROLE OF EDGE INTEGER Q SURFACES IN THE ITB FORMATION.

In addition to revealing the role played by integer rational q surfaces in the plasma interior, the heating timing scan is also a very useful tool to study the ITB triggering itself. When the additional heating is applied during the current ramp-up phase, the plasma internal inductance (l_i) starts to fall (fig 6a), indicating the accumulation of edge current due to the increase of the electron temperature and consequent decrease of the plasma resistivity. At this stage we define q_{edge} as in reference 19, which is roughly $q_{\text{edge}}=1.2 q_{95}$ for this type of plasma configuration where q_{95} is the safety factor at 95% of the outermost flux surface. As q_{edge} approaches integer values, such as 5, the edge current destabilises an external $n=1$, $m=q_{\text{edge}}$ MHD mode. This can be seen on figure 6a which shows the growth and decay of the $n=1$ component when q_{edge} crosses $q=5$ for

l_i close to 0.7. Although this edge mode has a small amplitude $\left(\frac{\tilde{B}_\theta}{B_\theta} \approx 2 - 5 \cdot 10^{-4} \right)$, it is observed

on the $n=1$ component of the magnetic fluctuations for many discharges forming an ITB. The low frequency of this $n=1$ mode (500Hz to 1kHz as measured by the $n=1$ frequency meter) is consistent with its location near the plasma edge. From these mode characteristics, it is possible to estimate that the amplitude of the edge magnetic perturbation corresponds to a displacement of the order of 0.5 to 2 cm at the outboard plasma mid-plane.

From the analysis of electron temperature data from ECE, it appears that the ITB is triggered simultaneously with the mode (at 4.1s), as illustrated by the increase in the neutron rate on figure 6a and by the temperature profile evolution in figure 6b. The criterion in ρ^*_{T} confirms that the trigger time of the ITB coincides with the edge $n=1$ MHD event. The criterion is compared with the $q=2$ evolution from EFIT and the $q_{\text{edge}}=5$ crossing time for a different discharge in figure 7. It confirms that the ITB forms close to the $q=2$ surface and that this coincides with q_{edge} crossing 5 and the peak of the MHD $n=1$ component at the plasma edge. Figure 7 also suggests that the barrier follows the evolution of the $q=2$ surface. Although this looks to be generally true in low magnetic shear JET Optimised Shear discharges, it does not necessarily imply that the triggering physics is governing the subsequent evolution of the ITB.

To confirm the correlation and the causality between the edge MHD mode and the onset time of the ITB, a database of more than 40 discharges has been developed with different plasma current ramp-up rate (from 0.37MA/s to 0.45MA/s). These data have also been complemented with a few 3.4T pulses. Using the ITB criterion for the determination of the ITB emergence time, the whole data set has been analysed to verify the link with the edge MHD activity each time it was observed as an the $n=1$ mode. The edge $n=1$ MHD onset time has been taken as the peak in root mean square level of the $n=1$ magnetic fluctuation (4.1s in the case shown on figure 6a). The ITB onset time is seen to be well correlated with the edge MHD event (fig 8) indicating the causal role played by the external MHD mode in the ITB triggering.

Using the same database it is also interesting to mark the range of q edge values at which barriers emerge. It can be seen (fig 9) that the ITB formation time is closely linked with the integer q ($q_{\text{edge}}=6$, $q_{\text{edge}}=5$ or $q_{\text{edge}}=4$) penetrating into the plasma as the plasma current is increased. As a result, the edge MHD mode, associated with an integer q_{edge} , seems to be the trigger of the ITB formed near the $q=2$ surface.

The above experimental analysis strongly suggests a link between the triggering of the ITB and the MHD on the outermost integer q surface driven by the accumulation of edge current in the current ramp-up phase as the main heating pulse is applied. Given the q_{edge} and internal inductance values, an external kink instability is likely to develop when an integer q surface is close to the edge [20]. Therefore, these observations combined with results from the previous section indicate that this edge MHD, coupled to MHD at $q=2$ or 3, is at the origin of the of ITB trigger.

THEORY CONSIDERATIONS AND DISCUSSION

The coupling between MHD activity at the plasma edge ($q=4, 5$ or 6) and at the internal $q=2$ or 3 surface can result from toroidicity, shaping and pressure induced (Shafranov) shifts of the magnetic flux surfaces. To investigate this coupling, calculations have been performed using the CASTOR resistive MHD code [21]. The CASTOR code solves the full linear resistive MHD equations for arbitrary aspect ratio and plasma shape. Although resistive MHD is not thought to be a wholly applicable model in the situation studied (e.g. which is not in the appropriate collisionality regime and where resistive layer widths are small compared with the gyro-radii), the calculations presented do give a useful indication of the possible mode coupling between the edge kink mode and the $q=2$ surface.

For these computations, typical equilibria have been used from the TRANSP interpretative modelling [22] of JET discharge 47667. This discharge exhibits a prompt ITB similar to pulse 47620 (figs 6a and 6b) with a target q_0 close to 2, and a peak neutron rate of $1.4 \cdot 10^{16}$ neutrons per second. Because of the lack of edge current measurement, TRANSP does not compute the edge current density profile very precisely. In the CASTOR simulation, the current density at the plasma edge has been therefore modified to reproduce the accumulation of edge current as the plasma current is ramped: with a value of $\langle J_{95} \rangle / J_{\max} = 0.17$ chosen to destabilise the observed edge kink mode. To examine the sensitivity of $n=1$ stability to the edge- q , the equilibrium is scaled in a self similar manner [23], which for the narrow range of scaling used here is approximately equivalent to scaling the q -profile by a constant.

The results of this q_{edge} stability scan are shown in figure 10. A comparison with the ideal growth rate (resistivity $\eta=0$), calculated with the MISHKA code [24], is also given in figure 10 and shows the strong edge kink mode destabilisation which occurs at $q_{\text{edge}} \sim 5$. It can be seen that the resistive mode for $\eta=10^{-6}$ and 10^{-8} extends the q_{edge} domain where the external kink mode grows to slightly higher q_{edge} . Here the resistivity is normalised as: $\frac{\eta}{\mu_0 \cdot R_m \cdot V_A}$ where V_A is the Alfvén velocity. In the resistive domain relatively strong coupling can occur between the edge kink and the internal rational surfaces, as shown in figure 11. For example for q_{edge} in the range of 4.9 to 5, the ratio of the $q=2$ island width to the edge displacement varies from about $1/5^{\text{th}}$ to $1/3^{\text{rd}}$ for $\eta=10^{-8}$. For $\eta=10^{-7}$, this ratio becomes about 40% larger. (For computational reasons, the edge displacement, which is chosen to be ~ 1 cm, is evaluated on the last perturbed magnetic flux surface which remains within the original plasma equilibrium boundary).

It should be noted that for these simulations $\beta=0$ is assumed. This assumption is made because while the layer physics model in CASTOR (resistive MHD) contains the curvature stabilisation term which tends to suppress tearing modes at representative β_p and resistivity, the destabilising terms such as bootstrap effects, and non-linear effects, are not included. The fact that large $m=2, n=1$ islands are sometimes observed in discharges where ITBs fail to trigger (see figure 4), confirms that islands can be destabilised. The CASTOR model does, however, reproduce

the external (Δ') solution for the tearing mode stability and so correctly treats the mode coupling between integer- q surfaces.

Experimentally, signs of mode coupling have been observed on the fast sampled magnetics data. In some cases the toroidal and poloidal structure of the external $n=1$ $m=q_{\text{edge}}$ mode is strongly altered when the barrier forms, suggesting that coupling takes place at this time. Simultaneously, an $m=2$ $n=1$ perturbation has also been detected close to the 'foot-point' of the barrier using the correlation between edge magnetic fluctuations and electron temperature fluctuations from ECE, indicating the possible presence of an island at the foot of the barrier.

The strong poloidal mode coupling of the external kink mode to the $q=2$ and $q=3$ rational surfaces indicates the potential for modifying transport and plasma flows at the internal rational q surfaces. However, the effect of toroidal flow shear between the edge and internal rational q surfaces should also be considered; the edge MHD is measured to have a frequency of ~ 0.5 to 1kHz, whereas, at the $q=2$ surface it has a frequency of ~ 5 kHz. This flow shear acts to inhibit tearing at more than one rational surface [25], until a threshold in magnetic field perturbation is exceeded. Previous experiments using the internal saddle coils in JET to simulate such a field [26], have measured the threshold of the (2,1) perturbation to induce a $q=2$ island in similar plasma conditions. The threshold is found to decrease by a factor of 2 as the internal inductance decreases from 1.1 (standard discharges) to 0.7 (optimised shear discharges). This threshold will be higher when the ITB forms (due to the torque from the neutral beams). But even if the threshold to produce an $m=2$, $n=1$ island is not exceeded there will be a magnetic 'braking' effect at $q=2$, as predicted theoretically [27], and found experimentally on DIII-D [28]. It is possible that the resulting local changes in plasma flow at $q=2$ are sufficient to trigger the ITB by increasing the EXB shearing rate which, in-turn, stabilises the turbulence and triggers the creation of a transport barrier. Local radial transport losses resulting from the modification of the field line topology is another possibility to change the EXB shearing rate in the vicinity of the rational q surfaces.

CONCLUSIONS

The JET Optimised Shear Regime experiments studied in this paper have been mainly performed in conditions where small amounts of pre-heating (0 to 2MW of ICRH) are applied in the current ramp-up phase prior to the heating pulse. In these conditions, it is observed that the formation of 'strong' ITBs is very sensitive to the start time of main heating. ITBs form in regions of low positive magnetic shear in the vicinity of rational q surfaces, $q=2$ or $q=3$. In addition, experimental analysis indicates that the rational surface follows the ITB in its evolution as the barrier expands, and is located at the 'foot-point' of the barrier. These characteristics suggest that the MHD at the integer q surfaces could provide the trigger for the ITB formation.

The ITB emergence is also well correlated with edge $n=1$ MHD. This is most likely to be the consequence of a large edge current density when the plasma current is ramped up in presence of strong additional heating. An external kink mode is then destabilised as an integer q surface ($q=4$, $q=5$ or $q=6$) enters the plasma. Since ITBs are formed in the vicinity of internal integer q

surfaces, toroidal mode coupling is the most plausible candidate mechanism to explain the link between the edge MHD occurrence and the ITB emergence time.

In these experimental conditions, simulations with the CASTOR code indicate that strong mode coupling can occur between the edge MHD mode and the internal q surface. The destabilisation of the MHD at $q=2$ or $q=3$ by the coupling process could provide a locally enhanced shear in the plasma flow by ‘mode braking’ (as described in reference 25 and 28, for instance), and act as a trigger for the ITB formation. It is also possible that topological modifications resulting from the internal MHD assist in the ITB triggering process.

Other experimental and theoretical studies have suggested different mechanisms relying on a local reduction in transport associated with low order rational q surfaces [14, 29] to explain the link between rational q surfaces and ITBs. However, these studies do not address the triggering of internal barriers by external influences such as mode ‘braking’.

The role of these external influences is crucial for understanding the required power to trigger ITBs for next step devices. The above studies strongly suggest that MHD destabilised at the plasma edge is the drive for the bifurcation to improved core confinement. This drive appears to reduce the additional heating power required to trigger the ITB (power threshold) compared with the ‘natural’ condition without any trigger. Other types of MHD trigger have also been observed with fishbone-like characteristics in ASDEX-Upgrade for example [30]. MHD triggers are not necessarily the only means to trigger an ITB, and recent experiments suggest that laser ablation or shallow pellets may also fulfil a similar role. In JET positive shear experiments, however, the edge MHD, when present, is correlated with the barrier emergence. Ultimately, the control of these mechanisms should contribute to the control of ITBs, an indispensable tool for an advanced tokamak reactor.

ACKNOWLEDGEMENTS

The authors gratefully acknowledge the work of N. Hawkes (UKAEA Fusion) in providing the q profile reconstructions used in this paper. The analysis of the ITB database made by G. Tresset (CEA Cadarache) has also been essential in assisting the work in this paper. This work has been performed within both the frame work of the JET Joint Undertaking and European Fusion Development Agreement (EFDA). The UKAEA authors were jointly funded by the UK Department of Trade and Industry and EURATOM.

REFERENCES

- [1] E J Strait, et al, Phys. Rev. Lett. **75** (1995) 4421.
- [2] T.Fujita et al. Proc. in Fusion Energy (16th Int. Conf. MontrÈal 1996), IAEA, Vienna, Vol. I (1997) 227.
- [3] M. Bell, et al., Plasma Phys. and Control. Fusion, **41**, (1999) A719.
- [4] Equipe Tore Supra, presented by X. Litaudon, Plasma Phys. Control. Fusion **38** (1996) A251.

- [5] R C Wolf, et al, in Fusion Energy, (Proc. 17th Int. Conf. Yokohama 1998), IAEA, Vienna, Vol. II (1999) 773.
- [6] JET Team, Proc. in Fusion Energy (16th Int. Conf. MontrÈal 1996), IAEA, Vienna, Vol. I (1997) 487.
- [7] C. Gormezano, et al., Plasma Phys. Control. Fusion, **41**, (1999) B367.
- [8] G D Conway, et al., Phys. Rev. Lett. **84** (2000) 1463.
- [9] T.S. Hahm, K.H. Burrell, Phys. Plasmas **2** (1995) 1648
- [10] T J J Tala, et al, Plasma Phys. Control. Fusion, **43**, (2001) 507.
- [11] C D Challis et al., Plasma Phys. Control. Fusion, **43**, (2001) 861.
- [12] Y Koide, et al, Phys. Rev. Lett. **72** (1994) 3662
- [13] C M Greenfield, et al, in Fusion Energy (Proc. 17th Int. Conf. Yokohama 1998, IAEA, Vienna, Vol. II (1999) 69.
- [14] G M D Hogeweyj, et al, Nucl. Fusion **38** (1998) 1881
- [15] A C C Sips et al., Plasma Phys. Control. Fusion **40** (1998) 1171
- [16] G. Tresset, X. Litaudon, D. Moreau, X. Garbet and contributors to the EFDA-JET work programme, JET-EFDA-PR(00)09, submitted to Nuclear Fusion.
- [17] N C Hawkes, et al, Rev. Sci. Instrum. **70** (1999) 894
- [18] D P O'Brien, et al, Nucl. Fusion **32** (1992) 1351.
- [19] Yoshino et al, Proc. in Plasma Physics and Controlled Nuclear Fusion Research (Proc 14th Int. Conf. Würzburg 1992), IAEA, Vienna, Vol III, 1993, 405.
- [20] J A Wesson, Nuclear Fusion **18**, (1978) 87.
- [21] W. Kerner, J.P. Goedbloed, G.T.A. Huysmans, S. Poedts and E. Schwartz J. Comp. Physics **142**, (1998) 271.
- [22] Budny, R.V., et al., Nucl.Fusion **32** (1992) 429.
- [23] S. Poedts, H.A. Holties, J.P. Goedbloed et al, 'HELENA Installation and User Guide', Rijnhuizen report, 96-228 (1996).
- [24] A B Mikhailovskii, G T A Huysmans and W O K Kerner et al, Plasma Phys Rep, **23** (1997) 844
- [25] R Fitzpatrick and T C Hender, Phys Fluids **B3** (1991) 644
- [26] R.J. Buttery et al, Nucl Fusion **40** (2000) 817
- [27] T C Hender et al, Nucl Fusion **32** (1992) 2091
- [28] R J LaHaye et al, Phys of Plasmas, **1** (1994) 373
- [29] A Thyagaraja, Plasma Phys. Control. Fusion, **42**, (2000) B255.
- [30] O. Gruber et al., Plasma Phys. Control. Fusion, **42**, (2000) 117.

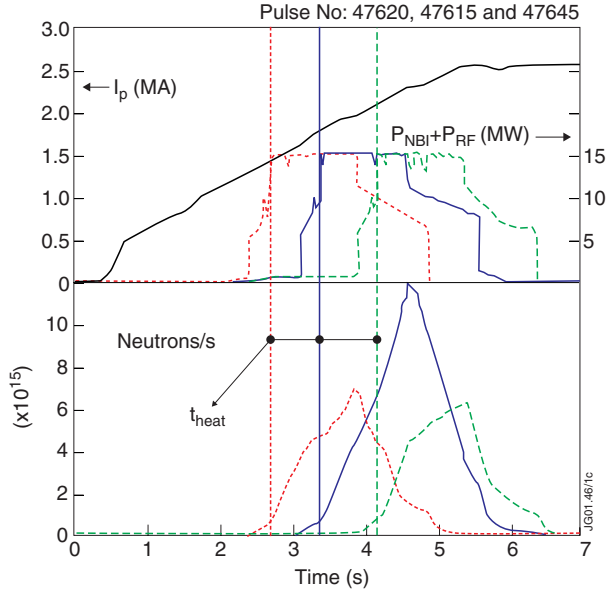


Fig.1: Neutron rate evolution for the timing scan experiment. All three discharges form an Internal Transport Barrier. Highest neutron yield is obtained for $t_{\text{heat}}=3.4\text{s}$.

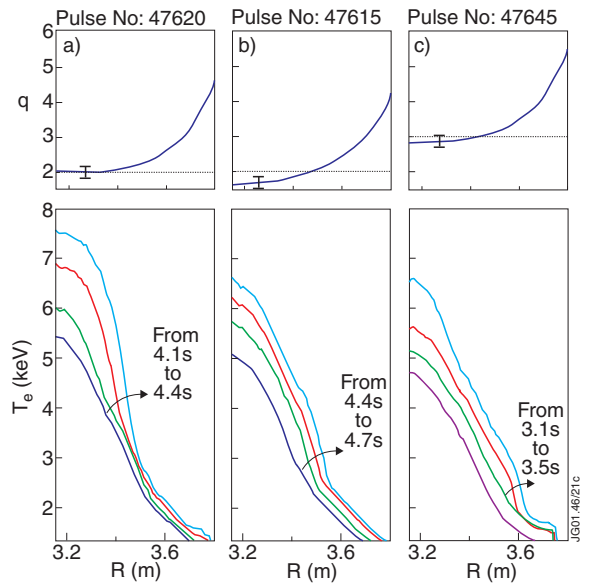


Fig.2: Temperature profiles from ECE measurement at the barrier formation. a) middle timing ($t_{\text{heat}}=3.4\text{s}$), b) late timing (4.2s), c) early timing (2.6s). Arrows are indicating the evolution of the ITBs with time for each three cases.

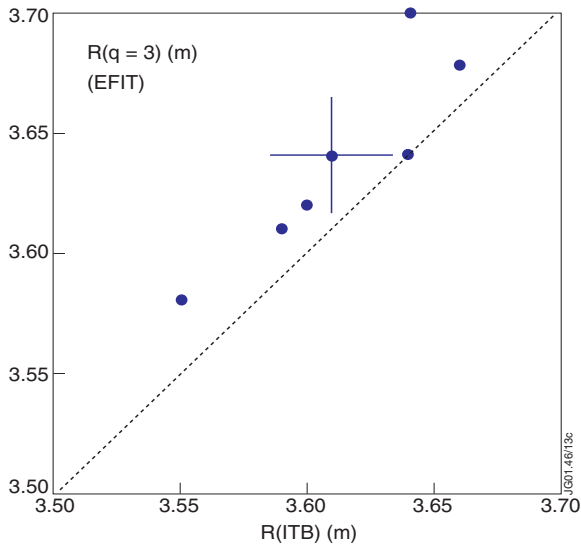


Fig.3: Position of the $q=3$ surface with respect to the foot of the barrier for "wide" $q=3$ Internal Transport Barrier determined from the ITB criterion. The data include 2.6T and 3.4T pulses.

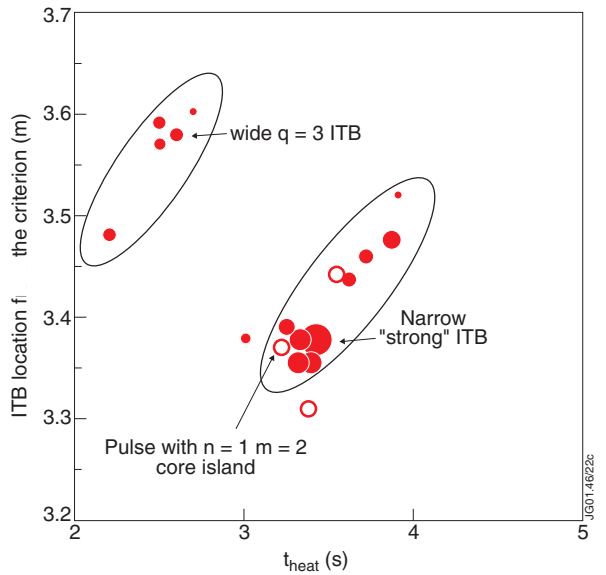


Fig.4: Location of the ITB versus the t_{heat} for timing scan pulses with the same density ($\langle n_e \rangle = 1.10^{19} \text{m}^{-3}$), toroidal field (2.6T) and additional power (10.5MW NBI and 4.5MW ICRH). The radius of the circles is proportional to the maximum neutron yield reached by each discharge. Open circles are pulses local flattening on T_e profile associated with the presence of a core $q=2$ island confirming that the $q=2$ flux surface enters the plasma for t_{heat} close to 3.3s . For these discharges, major radius is given by the location of the $m=2, n=1$ perturbation.

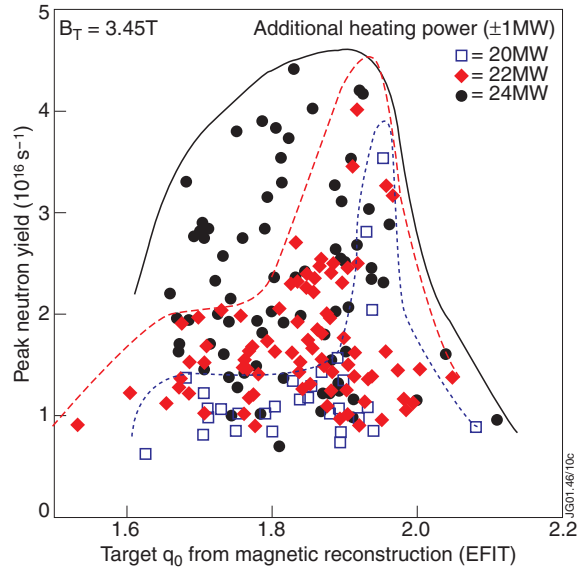


Fig.5: Neutron yield versus q_0 for 3.4T database of pulses with different input power. The lines are enveloping three different domains of input power. At 20MW (opened squares) strong barriers can be formed in a narrow range of target q when q_0 is close to 2. At higher power 22MW (diamonds) and 24MW (filled circles), the domain of existence is less sensitive to the value of q_0 .

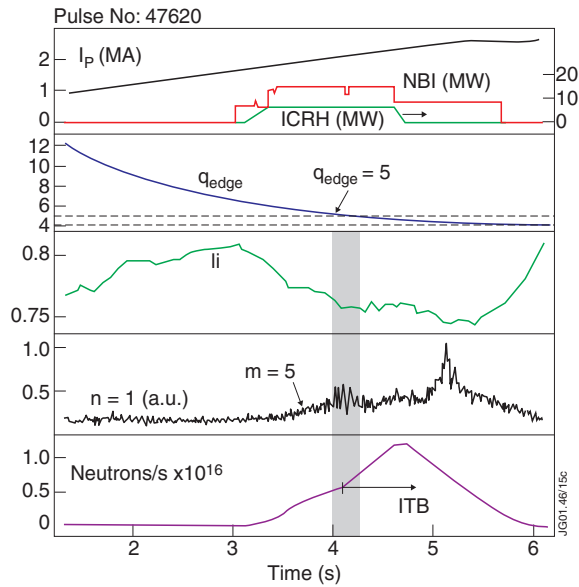


Fig.6: (a) Correlation of the MHD associated with the plasma edge with the ITB emergence for pulse 47620. When the additional heating is applied, the edge current builds up and destabilises edge MHD when integer $q_{edge}=5$ penetrates into the plasma. The ITB is triggered at the time of the MHD activity peaks at 4.1s.

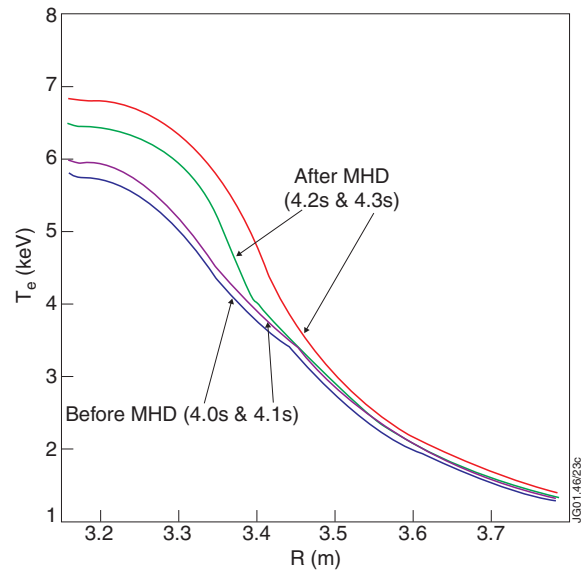


Fig.6: (b) T_e profile evolution before and after the MHD event when $q_{edge}=5$ appears near the plasma edge.

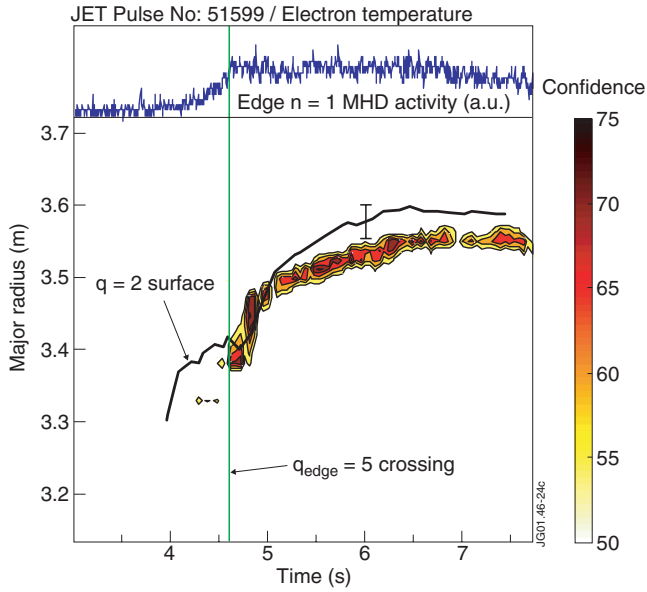


Fig.7: ITB criterion for pulse 51599 using electron temperature from ECE. The contour lines are confidence lines as calculated by the ρ^*/LT criterion (50% corresponds to the threshold value of $1.4 \cdot 10^{-2}$ for ITB existence). The evolution of the $q=2$ surface is also overlaid on the same graph as well as the edge MHD and the time of $q_{\text{edge}}=5$ crossing. All these events show good correlation at 4.6s.

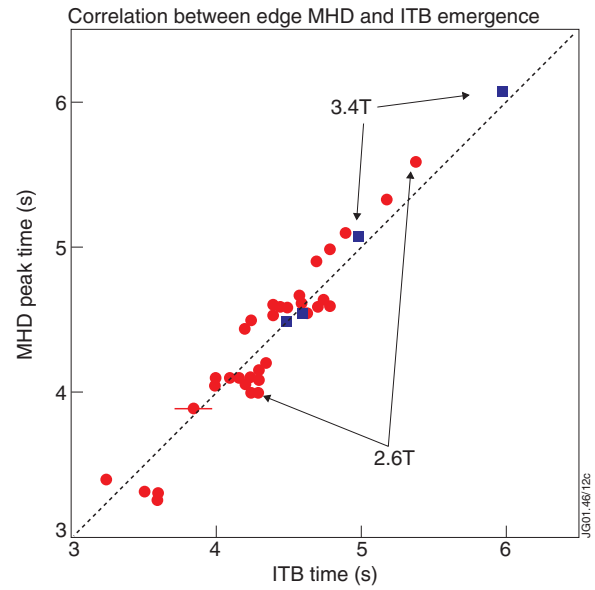


Fig.8: Correlation of the ITB emergence time from the ITB criterion with the integer q edge crossing for a set of 2.6T (small circles) and 3.4T discharges (open large circles)

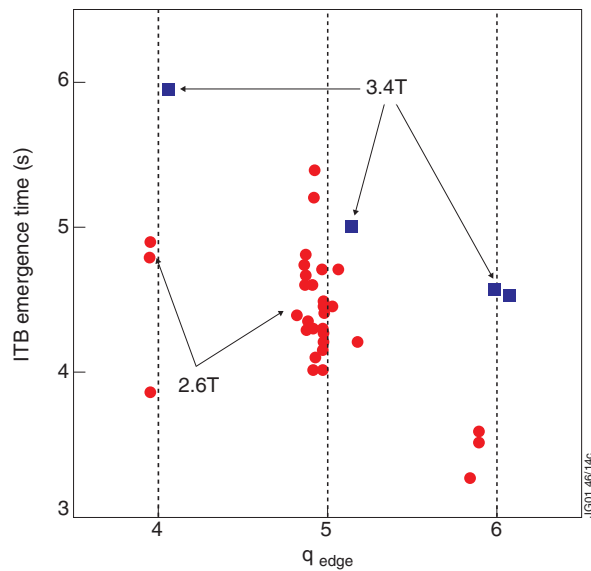


Fig.9: Correlation of the ITB emergence time from the ITB criterion and the MHD peak time for the same data set as figure 8.

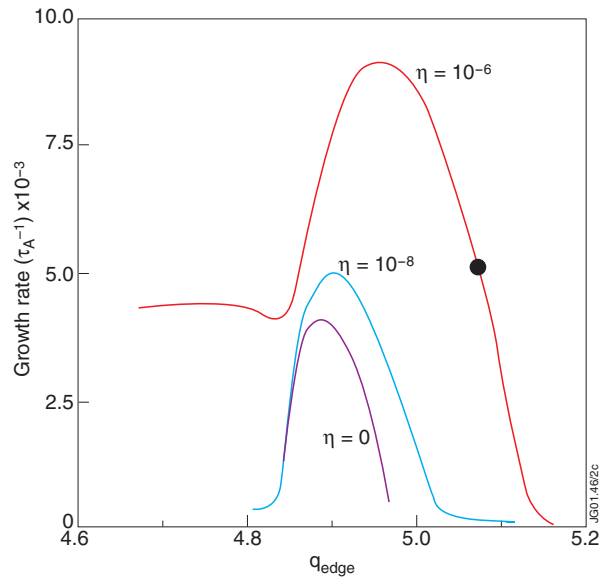


Fig.10: Growth rate as a function of q_{edge} and for various values of normalised resistivity. The edge current gives rise to an $n=1$ mode whose stability depends strongly on the edge q . The dot on the 10^{-6} resistivity curve indicates the position at which the field line plot (figure 11) is made.

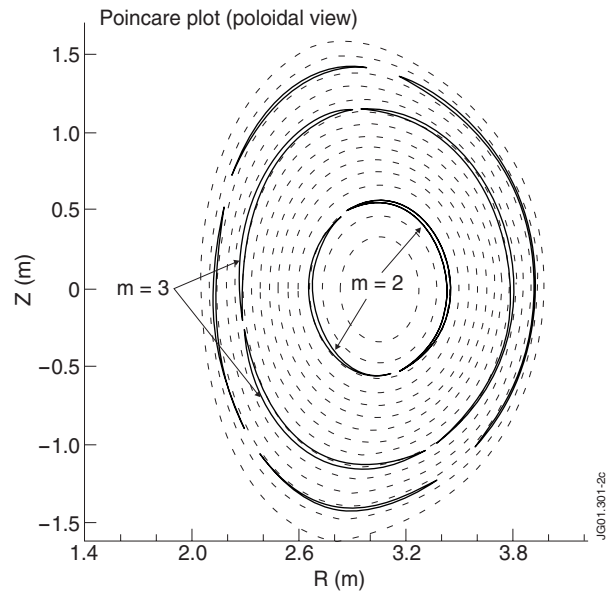


Fig.11: Field line plot showing $m=2, 3$ and 4 islands for normalised resistivity of 10^{-6} and $q_{edge}=5.08$ as indicated by the dot on figure 10.